Inorg. Chem. **2007**, *46*, 8739–8745

Synthesis, Structure, and Unexpected Magnetic Properties of $La_3Re_2O_{10}$

Heather L. Cuthbert,*[†,‡] John E. Greedan,[†,‡] Ignacio Vargas-Baca,[‡] Shahab Derakhshan,[†,‡] and Ian P. Swainson[§]

Department of Chemistry, McMaster University, Hamilton, Ontario, Canada, L8S 4M1, Brockhouse Institute for Materials Research, McMaster University, Hamilton, Ontario Canada, L8S 4M1, Canadian Neutron Beam Centre, National Research Council, Chalk River Laboratories, Chalk River, Ontario, Canada, K0J 1J0

Received May 24, 2007

The compound $La_3Re_2O_{10}$ has been synthesized by solid-state reaction and characterized by powder neutron diffraction, SQUID magnetometry, and heat capacity measurements. Its structure consists of isolated $[Re_2O_{10}]^{9-}$ dimer units of two edge-shared ReO_6 octahedra, separated by La^{3+} within the lattice. The Re–Re distance within the dimer units is 2.488 Å, which is indicative of metal–metal bonding with a bond order of 1.5. The average oxidation state of the Re atom is +5.5, leaving one unpaired electron per dimer unit ($S = 1/2$). Although the closest interdimer distance is 5.561 Å, the magnetic susceptibility data and heat capacity measurements indicate this compound exhibits both short- and long-range magnetic order at surprisingly high temperatures. The zero field cooled (ZFC) magnetic susceptibility data show two broad features at 55 and 105 K, indicating short-range order, and a sharper cusp at 18 K, which signifies long-range antiferromagnetic order. The heat capacity of $La_3Re_2O_{10}$ shows a λ-type anomaly at 18 K, which is characteristic of long-range magnetic order. DFT calculations determined that the unpaired electron resides in a π-bonding orbital and that the unpaired electron density is widely delocalized over the atoms within the dimer, with high values at the bridging oxygens. Extended Hückel spin dimer calculations suggest possible interaction pathways between these dimer units within the crystal lattice. Results from the calculations and fits to the susceptibility data indicate that the short-range magnetic ordering may consist of 1-D antiferromagnetic linear chains of coupled $S = 1/2$ dimers. The magnetic structure of the antiferromagnetic ground state could not be determined by unpolarized neutron powder diffraction.

Introduction

The magnetic properties of oxides involving the 4d and 5d transition metals have been much less explored in comparison to the 3d elements. The crystal chemistry and structures of the 4d and 5d oxides are often different due to the more extended nature of the 4d and 5d orbitals, the occurrence of higher oxidation states, and the tendency to form metal−metal bonds. These factors can have a detrimental effect on the resulting magnetism; however, novel magnetic properties are also possible.

There are a few known oxides involving lanthanum and rhenium, and many of these contain multiple Re−Re bonds. Of course, in compounds such as La_3ReO_8, rhenium is in its maximum oxidation state and metal−metal bonding does not occur.[1,2] Instead, Re(VII) ions are found in isolated octahedral sites. In contrast, $La_4Re_2O_{10}$ consists of isolated $[Re_2O_8]^{8-}$ units, linked together by La^{3+} ions.[3] The very short Re−Re bond length of 2.259(1) Å is attributed to a triple bond, pairing all electrons. A study of various Re(IV) oxides demonstrated that they can be oxidized and reduced; however, the exact structures of the products were not determined.[4]

In addition, oxides exist with rhenium in a mixed oxidation state. In $La_6Re_4O_{18}$, the average oxidation state of rhenium is +4.5.[5] Two different, isolated Re−Re-bonded clusters exist: $[Re_2O_8]^{8-}$ and $[Re_2O_{10}]^{10-}$, with Re−Re bond lengths

* To whom correspondence should be addressed. E-mail: cuthbehl@mcmaster.ca. Fax: 1-905-521-2773.
[†] Department of Chemistry, McMaster University.
[‡] Brockhouse Institute for Materials Research, McMaster University
[§] Chalk River Laboratories.

(1) Baud, G.; Besse, J.-P.; Chevalier, R.; Gasperin, M. *J. Solid State Chem.* **1979**, *29*, 267−272.
(2) Rae-Smith, A. R.; Cheetham, A. K.; Fuess, H. *Z. Anorg. Allg. Chem.* **1984**, *510*, 46−50.
(3) Waltersson, K. *Acta. Crystallogr.* **1976**, *B32*, 1485−1489.
(4) Baud, G.; Capestan, M. *Bull. Soc. Chim. Fr.* **1968**, *10*, 3999−4004.

10.1021/ic701011r CCC: $37.00
Published on Web 09/14/2007

of 2.235(6) and 2.456(5) Å, respectively, consistent with triple and double bonds. In all of these cases, the metal−metal bonding pairs the electrons within the Re dimers and the result is diamagnetism. However, in $La_4Re_6O_{19}$, with Re in the +4.333 state, a three-dimensional framework of edge-shared octahedral dimers that share corners is formed.[6,7] Despite the existence of metal−metal double bonds (Re−Re distance of 2.42 Å), this compound is metallic, indicating the presence of unpaired but delocalized electrons.

The title compound has been synthesized previously in single crystal-form using a hydrothermal method.[8] An unidentified powder was also a product. Its structure is comprised of isolated $[Re_2O_{10}]^{9-}$ dimeric units of two edge-shared ReO_6 octahedra, separated by La^{3+} within the lattice. The Re−Re distance within the dimer units was reported as 2.484(1) Å, consistent with metal−metal bonding. The average oxidation state of the Re is +5.5, leaving one unpaired electron per dimer unit ($S = 1/2$). Semiconducting behavior was observed, indicating localization of the electrons and the possibility of magnetism. However, the reported effective magnetic moment of about 6 μ_B at room temperature for $La_3Re_2O_{10}$ ($S = 1/2$) does not appear to make much physical sense, given the maximum spin-only effective moment for this system should be 1.73 μ_B.

The present report focuses on the synthesis of $La_3Re_2O_{10}$ using conventional solid-state methodologies for the first time, as well as a comprehensive study of its structure by powder X-ray and neutron diffractometry and its magnetic properties, utilizing SQUID magnetometry and heat capacity measurements.

Experimental Methods

Synthesis. $La_3Re_2O_{10}$ was synthesized by solid-state reaction, according to the following.

$$9La_2O_3 + 11ReO_3 + Re \rightarrow 6La_3Re_2O_{10} \quad (1)$$

Stoichiometric amounts of the starting reagents, La_2O_3 (99.9%, Aldrich, heated at 900 °C overnight before use), ReO_3 (Rhenium Alloys), and Re (Rhenium Alloys) were accurately weighed, ground together, pressed into a pellet and placed into a platinum crucible, which was sealed in a quartz tube under vacuum ($\sim 10^{-5}$ Torr). The reactants were heated to 1050 °C in a tube furnace and held for 48 h. The product obtained was a black powder.

X-ray and Neutron Diffraction. X-ray diffraction data were collected using a Guinier-Hagg camera with Cu Kα_1 radiation ($\lambda = 1.5406$ Å) and high-purity silicon powder as an internal reference. The reflections were recorded on photographic film, and the line intensities were converted to digital format using the KEJ LS-20 line scanner.

Variable-temperature powder neutron diffraction measurements were performed on the C2 diffractometer at the Canadian Neutron Beam Centre at Chalk River, Ontario. Data for crystal structure refinement (285 K) were collected at a wavelength of 1.32917 Å in the angular range of $12° \leq 2\theta \leq 113°$ with 0.1° steps. Similarly, data for investigation of the magnetic structure (4 and 285 K) were measured at a longer wavelength of 2.36957 Å in the range $5° \leq 2\theta \leq 85°$ with 0.1° intervals.

Magnetic Data. Magnetic measurements were collected using a Quantum Design SQUID magnetometer. Zero field cooled and field cooled (ZFC/FC) magnetic susceptibility data from 5 to 300 K and isothermal magnetization measurements from 0 to 5 T were recorded on a powder sample encased in a gelatin capsule. Diamagnetic corrections of 20×10^{-6} (La^{3+}), 16×10^{-6} (Re^{6+}), and 12×10^{-6} emu/mol (O^{2-}) were added to the susceptibility data. There was no diamagnetic correction for the sample holder.

Heat Capacity. Heat capacity data were measured from 5 to 115 K in zero applied field and from 5 to 30 K in a 9.0 T field using the heat capacity probe of the Oxford MagLab system. A suitable sample block was prepared by re-pressing and resintering a portion of the previously synthesized product. Sample structure integrity was verified by powder X-ray diffraction (Guinier). The thin block was mounted onto a sapphire measurement chip with Apeizon grease. Contributions to the measured heat capacity by the grease and sample chip were accounted for by the software.

Calculations. All DFT calculations described here were performed with the ADF 2004.01 density functional theory package.[9−11]

The calculation of model geometries was conducted using unrestricted calculations with the adiabatic local density approximation (ALDA) for the exchange−correlation kernel[12,13] and the differentiated static LDA expression was used with the Vosko−Wilk−Nusair parametrization.[14] Gradient corrections were performed with the exchange and correlation functionals of Perdew and Wang (PW91).[15] All basis functions had triple-ζ quality and were composed of uncontracted Slater-type orbitals (STOs), including frozen cores for O (1s), Re (4f), and La (4d) and two auxiliary basis set of STOs for polarization. Relativistic effects were modeled using ZORA.[16−18]

Extended Hückel spin dimer analysis using the CAESAR computational package was also performed to estimate the relative strength of the different interdimer exchange interactions.[19] Double-ζ STOs were used for Re d and O s and p orbitals.

Results and Discussion

Structural Characterization. The crystal structure of the compound was first verified from Guinier powder data. The obtained pattern and lattice constants matched well with the

(5) Besse, J.-P.; Baud, G.; Chevalier, R.; Gasperin, M. *Acta. Crystallogr.* **1978**, *B34*, 3532−3535.
(6) Morrow, N. L.; Katz, L. *Acta. Crystallogr.* **1968**, *B24*, 1466−1471.
(7) Sleight, T. P.; Hare, C. R.; Sleight, A. W. *Mat. Res. Bull.* **1968**, *3*, 437−444.
(8) Torardi, C. C.; Sleight, A. W. *J. Less-Common Met.* **1986**, *116*, 292−299.
(9) Velde, G. t.; Bickelhaupt, F. M.; Gisbergen, S. J. A. v.; Guerra, C. F.; Baerends, E. J.; Snijders, J. G.; Ziegler, T. *J. Comput. Chem.* **2001**, *22*, 931−967.
(10) Guerra, C. F.; Snijders, J. G.; Velde, G. t.; Baerends, E. J. *Theor. Chem. Acc.* **1998**, *99*, 391−403.
(11) *SCM, Theoretical Chemistry*; Vrije Universiteit: Amsterdam, The Netherlands, 2002.
(12) Gisbergen, S. J. A. v.; Snijders, J. G.; Baerends, E. J. *Phys. Rev. Lett.* **1997**, *78*, 3097−3100.
(13) Gisbergen, S. J. A. v.; Snijders, J. G.; Baerends, E. J. *J. Chem. Phys.* **1998**, *109*, 10644−10656.
(14) Vosko, S. H.; Wilk, L.; Nusair, M. *Can. J. Phys.* **1980**, *58*, 1200−1211.
(15) Perdew, J. P.; Chevary, J. A.; Vosko, S. H.; Jackson, K. A.; Pederson, M. R.; Singh, D. J.; Fiolhais, C. *Phys. Rev. B* **1992**, *46*, 6671−6687.
(16) Lenthe, E. v.; Baerends, E. J.; Snijders, J. G. *J. Chem. Phys.* **1993**, *99*, 4597−4610.
(17) Lenthe, E. v.; Baerends, E. J.; Snijders, J. G. *J. Chem. Phys.* **1994**, *101*, 9783−9792.
(18) Lenthe, E. v.; Ehlers, A.; Baerends, E. J. *J. Chem. Phys.* **1999**, *110*, 8943−8953.
(19) Ren, J.; Liang, W.; Whangbo, M.-H. *Crystal and Electronic Structure Analysis using CAESAR*, 2005; http://www.PrimeC.com/.

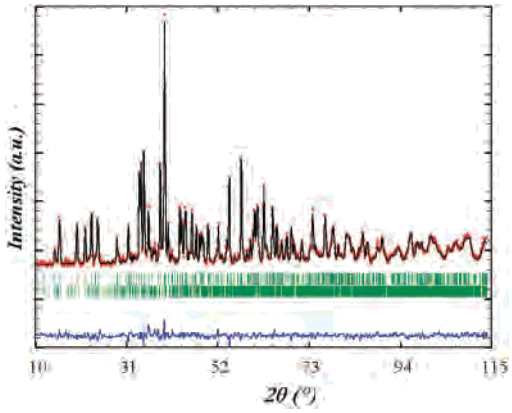

Figure 1. Rietveld refinement of the powder neutron diffraction data for $La_3Re_2O_{10}$. The circles are the experimental data, and the line is the calculated fit. The top set of tick marks denote the Bragg reflections of the $La_3Re_2O_{10}$ phase, whereas the bottom Bragg reflections are from the $La_6Re_4O_{18}$ impurity. The line at the bottom of the figure is the difference plot between the observed and calculated patterns.

previous single-crystal studies,[8] indicating the black powder produced was indeed $La_3Re_2O_{10}$. This work represents the first published preparation of $La_3Re_2O_{10}$ as a phase-pure polycrystalline powder using conventional solid-state methodologies.

Larger batches of the compound were synthesized for powder neutron diffraction measurements. Unfortunately, these samples contained some $La_6Re_4O_{18}$ impurity that was not present in the smaller batch preparation. Consequently, SQUID magnetometry and heat capacity measurements were performed on the pure powder material, whereas neutron diffraction data were collected using a combination of slightly impure powders.

Rietveld refinement of the powder neutron diffraction data was accomplished using FULLPROF,[20] with the crystal structure values as the model for $La_3Re_2O_{10}$ and the $La_6Re_4O_{18}$ impurity phase included. A plot of the refinement is shown in Figure 1. The overall agreement indices for the refinement were $R_p = 0.0308$, $R_{wp} = 0.0405$, and $\chi^2 = 1.34$. Agreement factors for the individual phases were $R_f = 0.0378$ and $R_B = 0.0200$ for $La_3Re_2O_{10}$ and $R_f = 0.0816$ and $R_B = 0.0320$ for $La_6Re_4O_{18}$. The relative weight percent of the impurity, calculated using the method of Hill and Howard,[21] was about 13%. Although this value is slightly high, the presence of $La_6Re_4O_{18}$ did not have a severe negative impact on the neutron data collected. This compound would not be magnetic due to the pairing of the Re electrons in metal−metal bonding.[5]

The crystal structure of $La_3Re_2O_{10}$ is shown in Figure 2. The basic structural unit is a $[Re_2O_{10}]^{9-}$ dimer of two edge-shared ReO_6 octahedra. These dimers are isolated from each other within the lattice by La^{3+} ions. The closest dimer−dimer distance is 5.561 Å. The lattice constants and selected interdimer bond lengths are displayed in Table 1.

The Re−Re bond length within the dimer is 2.488 Å, which is indicative of metal−metal bonding. Comparing this

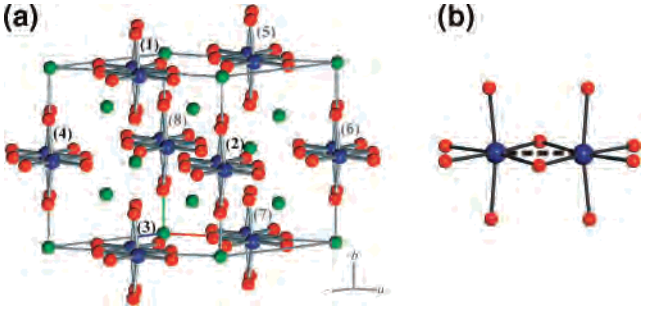

Figure 2. (a) Unit cell of $La_3Re_2O_{10}$. The atoms are designated by color: La (green), Re (blue), O (red). The numbers correspond to the selected interdimer distances reported in Table 1, as well as the magnetic coupling pathways considered in the calculations. (b) Detail of an individual $[Re_2O_{10}]^{9-}$ dimer unit, illustrating the metal−metal bond (dashed line).

Table 1. Lattice Constants and Selected Interdimer Distances for $La_3Re_2O_{10}$[a]

space group	*C*2/*m*	
a (Å)	7.8952(8)	[7.901(1)]
b (Å)	7.8340(8)	[7.866(1)]
c (Å)	7.1244(7)	[7.115(1)]
β (°)	115.208(4)	[115.44(1)]
	Intralayer (*ab* Plane) Distances	
1−2	5.561 Å	
1−3	7.834 Å	
2−4	7.895 Å	
	Interlayer Distances[b]	
1−5	7.124 Å	
1−8	7.598 Å	
2−8	8.073 Å	

[a] Literature values are shown in the brackets.[8] [b] The interlayer distances reported represent the distance between the same Re atoms of two different dimers.

distance with other halo-metal cluster systems, a bond order of 1.5 can be tentatively assigned.[22] The average oxidation state of Re in this complex is +5.5, implying that there are three electrons in each Re dimer, and the dimers are magnetic ($S = 1/2$ per dimer).

Magnetic Properties. The ZFC/FC magnetic susceptibility data collected from 2 to 300 K are plotted in Figure 3. The two curves diverge around 150 K. The ZFC data show two broad maxima centered at 105 and 55 K, respectively. These features are indicative of short-range order.

Attempts were made to fit the 55 K feature to various models of low-dimensional magnetic correlations. Considering the compound's crystal structure, probable models of this order would be either 1-D linear antiferromagnetic chains[23] or a 2-D antiferromagnetic square-planar lattice.[24] The analytical expressions derived from these models are both based on the general form of the spin−spin Hamiltonian (eq2):

$$H = -2\boldsymbol{J}\,\Sigma_{i<j}\,[S_x^i\,S_x^j + S_y^i\,S_y^j + S_z^i\,S_z^j] \qquad (2)$$

The 2-D fit failed to converge and, hence, was discarded. The 1-D Heisenberg $S = 1/2$ antiferromagnetic linear chain

(20) Roisnel, T.; Rodriguez-Carvajal, J. *Mater. Sci. Forum* **2000**, *378*−*381*, 118−123.
(21) Hill, R. J.; Howard, C. J. *J. Appl. Crystallogr.* **1987**, *20*, 467−474.
(22) Cotton, F. A. *Inorg. Chem.* **1965**, *4*, 334−336.
(23) Estes, W. E.; Gavel, D. P.; Hatfield, W. E.; Hodgson, D. J. *Inorg. Chem.* **1978**, *17*, 1415−1421.
(24) Navarro, R. In *Magnetic Properties of Layered Transition Metal Compounds*; Jongh, L. J. d., Ed.; Kluwer Academic Publishers: Dordrecht, 1990; pp 105−184.

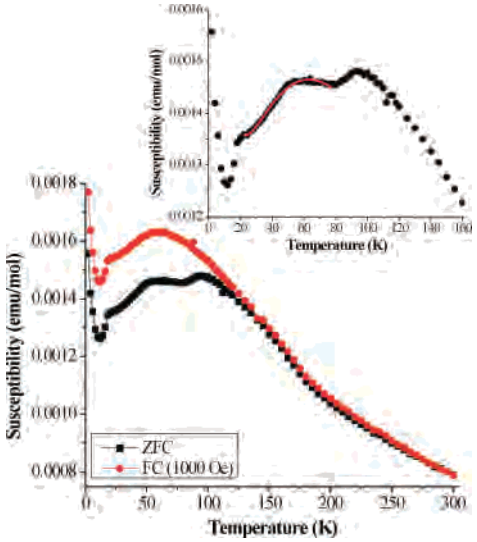

Figure 3. Zero field cooled/field cooled (ZFC/FC) magnetic susceptibility of $La_3Re_2O_{10}$. Inset: Fit of the low-temperature feature in the ZFC magnetic susceptibility data to a 1-D linear chain model. The circles are the experimental points, and the line is the fit.

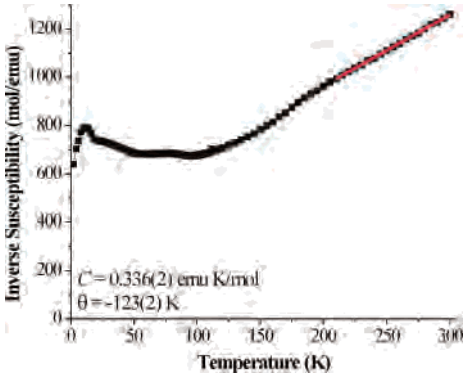

Figure 4. Fit of the ZFC magnetic susceptibility data from 200 to 300 K to the Curie−Weiss law.

model fit the data well, as seen in the inset of Figure 3. The *g*-factor found was 1.44(11), which is slightly low, and the magnitude of the exchange constant, $|J/k_B|$ was 51(1) K. A Curie−Weiss term and a temperature-independent paramagnetism term were included in the fit to model a low-temperature paramagnetic impurity, yielding values of $C = 1.2(1) \times 10^{-3}$ emu K/mol, $\theta = 11(5)$ K, and $3.1(2) \times 10^{-4}$ emu/mol, respectively.

Finally, a sharp cusp at 18 K can be found in the ZFC curve, followed by a large drop in the measured susceptibility, until very low temperatures when the susceptibility rises. This steep rise at low temperature can be attributed to a paramagnetic impurity. However, the 18 K feature could be indicative of the onset of long-range magnetic order.

A fit of the ZFC susceptibility data from 200 to 300 K to the Curie−Weiss law (eq 3) was performed and is pictured in Figure 4.

$$\chi = \frac{C}{T - \theta} \tag{3}$$

The Curie constant found was 0.336(2) emu K/mol, which is slightly below the calculated "spin only" value of 0.375 emu K/mol. This could indicate delocalization of the lone

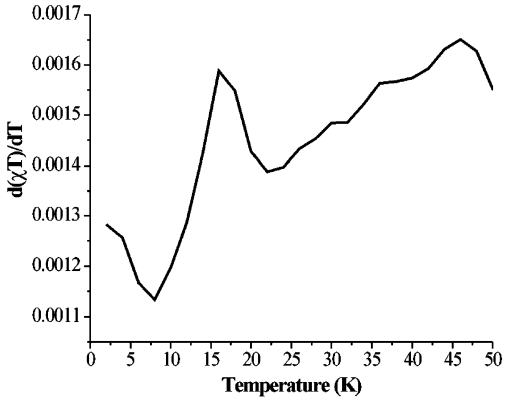

Figure 5. Fisher heat capacity of $La_3Re_2O_{10}$. The peak of the λ-like anomaly is ~17 K.

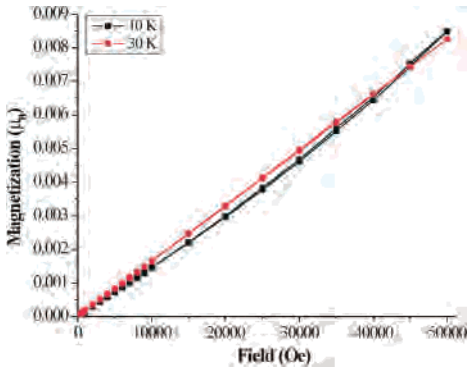

Figure 6. Isothermal magnetization curves for $La_3Re_2O_{10}$ collected below (10 K, squares) and above (30 K, circles) the critical temperature, T_c.

unpaired electron within the dimer unit or contribution of an orbital moment due to intradimer spin−orbit coupling. The Weiss temperature was −123(2) K, suggestive of dominant antiferromagnetic interactions. No temperature-independent paramagnetic term was needed due to the clear linearity of the data in this temperature range.

The temperature derivative of χT plotted against the temperature (T), the so-called "Fisher heat capacity",[25] is shown in Figure 5.

There is an anomaly present at lower temperature, but due to the sloping background, it is difficult to assign an exact value for the peak. However, it appears to be centered at about 17 K, which corroborates the idea from the magnetic susceptibility data that long-range magnetic order sets in around 18 K.

Isothermal magnetization measurements at 10 and 30 K were collected using fields between 0 and 5.0 T (Figure 6).

Neither curve approaches the expected saturation magnetization for a $S = 1/2$ compound of 1.0 μ_B. In addition, no significant hysteresis or remanent magnetization were observed. The 30 K data are linear, indicating paramagnetism; however, the 10 K data are significantly curved. This is consistent with the presence of an antiferromagnetic state at low temperatures with the field-induced curvature due to a spin flop transition.

Heat Capacity. The heat capacity of $La_3Re_2O_{10}$ measured from 5 to 24 K with no applied field is pictured in Figure 7.

(25) Fisher, M. E. *Philos. Mag.* **1962**, *7*, 1731−1743.

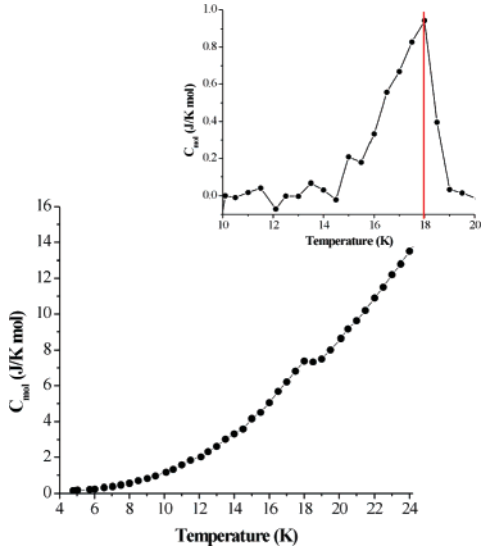

Figure 7. Heat capacity of $La_3Re_2O_{10}$, measured in the absence of a magnetic field. Inset: Heat capacity after subtraction of the lattice contribution. Note the λ-like anomaly at 18 K.

A distinct anomaly appears at ~18 K, indicative of long-range magnetic order, consistent with the susceptibility results. Application of a 9.0 T field had little effect, demonstrating the robustness of this magnetic feature. Unfortunately, a lattice match could not be synthesized. However, fitting both the low-temperature and higher-temperature data (well below and above the anomaly) to the expression:

$$C = \gamma T + \beta T^3 \tag{4}$$

leads to an estimation of the lattice contribution to the specific heat. Subtracting this function from the heat capacity data results in a more defined λ-like peak at 18 K (inset Figure 7).

The entropy associated with this magnetic transition can also be calculated from the heat capacity data. Integration of the area under the curve results in an estimation of the entropy loss according to:

$$\Delta S = \int_0^T (C_{\mathrm{mol}}/T)\, \mathrm{d}T \tag{5}$$

from which $\Delta S = 0.12$ J/K mol. The entropy loss expected for a magnetic transition is equal to $R \ln(2S + 1)$, and for $La_3Re_2O_{10}$, this would be 5.76 J/K mol. Although the measured magnetic entropy loss is only ~2% of the total entropy, this is not unreasonable, given the importance of short-range correlations present at much higher temperatures which would eliminate much of this entropy before the transition to long-range order.

Neutron Diffraction. The low-angle part of the neutron powder patterns obtained at 4 and 285 K, as well as a difference plot, is shown in Figure 8.

Despite over 60 h of data collection at low temperature, no magnetic reflections were observed. $La_3Re_2O_{10}$ is, of course, a very dilute magnetic system (the one unpaired electron is extensively delocalized over 15 atoms), and it may be impossible to detect the ordered moment using unpolarized neutrons. An alternative explanation is that the compound does not exhibit long-range magnetic order. However, the Fisher heat capacity (Figure 5), the field dependence of the magnetization (Figure 6), and the thermal heat capacity (Figure 7) all indicate long-range antiferromagnetic magnetic order below 18 K. It seems far more likely that the former explanation is correct.

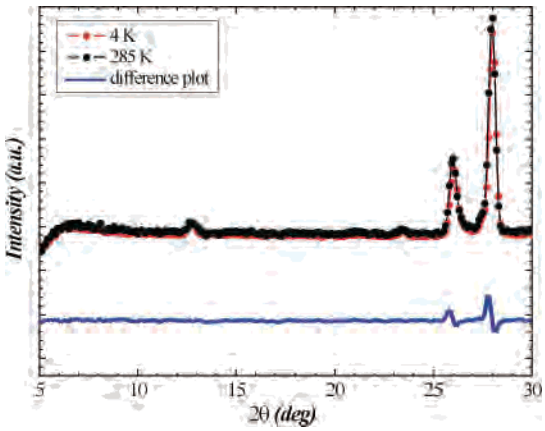

Figure 8. Comparison of the powder neutron diffraction patterns of $La_3Re_2O_{10}$ taken below (4 K) and above (285 K) the critical temperature, T_c, as well as a difference plot (lower line).

Computational Modeling. DFT computational modeling was undertaken to investigate the electronic structure of the isolated, paramagnetic dimer, especially the distribution of the electron density. As well, an attempt was made to determine the relative strengths of selected interdimer interactions using DFT and EHTB. As a first approximation, the electronic structure of the isolated dimer cluster was mimicked using the model compound $Re_2O_{10}H_8^-$ (C_{2h}). Only the positions of the capping hydrogen atoms were optimized. The metal ions are formally in oxidation states +5 and +6. There are three electrons available for metal−metal bonding—two occupy a σ-bonding orbital (a_g), and the unpaired electron is located in a π-bonding orbital (a_u). Both orbitals are shown in Figure 9a.

From the composition of the SOMO or the map of spin density (Figure 9b), it is clear that there is significant delocalization of spin over the oxygen atoms, in particular those bridging the rhenium metal ions. This suggests that the lanthanum ions bonded to the bridging oxygens are likely to enable interdimer spin coupling.

The bimetallic clusters are organized in layers within the *ab* plane, according to the crystal structure of $La_3Re_2O_{10}$ (Figure 2). Within each layer, three different coupling pathways are possible: 1−2, 1−3, and 2−4, with respect to the labeling system depicted in Figure 2. These, as well as additional interlayer interaction pathways, were examined using DFT with small molecular models that included two dimers at a time. The relative strength of the interaction between unpaired electrons is quantified by the magnitude of the spin−spin coupling constants, but their accurate calculation is only possible with highly correlated methods. Instead, the energy gap between the singlet and the triplet states can be used to estimate the coupling constants; the

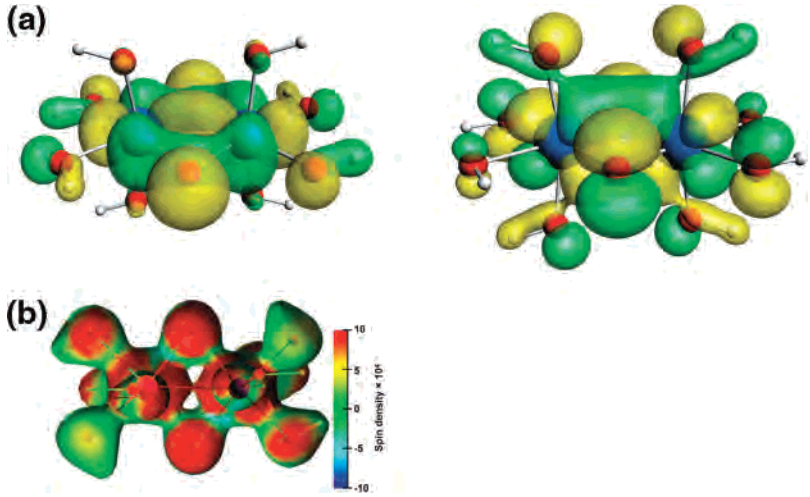

Figure 9. (a) Re−Re bonding orbitals of $Re_2O_{10}H_8^-$ as calculated using DFT. The picture on the left depicts the SOMO-1 or σ-bonding orbital, whereas the one on the right is the SOMO or π-bonding orbital (which is only half-filled). Legend of colors: Re (blue), O (red), H (white), orbital lobes (green, yellow). (b) Spin density for $Re_2O_{10}H_8^-$ mapped over the total density isosurface plotted at 0.05.

limitations of this approach and the accuracy of DFT methods have been examined before.[26−30]

In all of these calculations, the triplet states were consistently below the energy of the singlets. This would imply that the magnetic interaction between two dimers should be ferromagnetic. However, there is no experimental evidence for ferromagnetism. The observed magnetic behavior must be a consequence of extended interactions throughout the lattice that cannot be accounted for with this approach. Instead, extended Hückel, spin dimer analysis[31] was employed to assess the relative magnitude of the spin interactions. In this method, the intersite hopping energy, Δe, is calculated by comparing the energy gap between the highest occupied state and the lowest unoccupied state. Assuming that $J \approx -(\Delta e)^2/U$, where U is the Coulomb integral (and can be considered as constant for a given magnetic ion), the relative magnitude of the various magnetic exchange coupling constants, J, can be determined. Each $[Re_2O_{10}]^{9-}$ dimer is comprised of one half-filled electronic state. Accordingly, the exchange interactions between two of these dimers, in various directions, were investigated and the relative exchange energies are summarized in Table 2.

Within the *ab* plane, the 1−2 interaction is the strongest and the others are much weaker. This intralayer pathway is also the shortest. However, the strongest overall interdimer coupling, relative to all of the pathways examined, is the 1−8 dimer−dimer interaction. Surprisingly, this is an interlayer interaction, and is also not the shortest Re−Re interdimer contact (see Table 1). Dimer coupling between 1 and 8 would extend along the (1 1 2) direction and lead to short-range magnetic order consisting of 1-D antiferromagnetically coupled dimer chains. This finding is consistent with the fits to the broad feature at 55 K in the SQUID magnetometry data. The 1−2 interaction is weaker (about one-tenth the strength of the 1−8 pathway); however, coupling of the chains in the (1 1 0) direction is still highly probable. This could lead to the long-range magnetic order evident from SQUID magnetometry and heat capacity data.

Table 2. $(\Delta e)^2$ for Some of the Magnetic Exchange Pathways (Intralayer and Interlayer) between Different Dimers Calculated Using the Spin Dimer Model

	$(\Delta e)^2$ (meV)^2	relative	relative (overall)
	Intralayer Pathways		
1−2	68.3	1	0.12
1−3	2.78	0.041	0.0050
2−4	0.125	0.002	0.00022
	Interlayer Pathways		
1−5	11.27	0.020	0.020
1−8	569.6	1	1
2−8	26.8	0.047	0.047

Conclusions

The synthesis of $La_3Re_2O_{10}$ by solid-state reaction was successfully carried out for the first time, yielding a pure-phase black powder. Its magnetic properties were subsequently studied, revealing some interesting, unusual, and unexpected results.

Despite a distance of over 5 Å between isolated $S = 1/2$, $[Re_2O_{10}]^{9-}$ dimer units, evidence for both short- and long-range magnetic order at relatively high temperatures is clear from both SQUID magnetometry and heat capacity measurements. The short-range order appears to consist of 1-D linear chains of antiferromagnetically coupled dimers. This conclusion was reached by experimental fits to the magnetic susceptibility data and extended Hückel spin dimer calculations. These chains would most likely extend diagonally across the unit cell in the (1 1 2) direction, as this is the

(26) Mitani, M.; Yamaki, D.; Takano, Y.; Kitagawa, Y.; Yoshioka, Y.; Yamaguchi, K. *J. Chem. Phys.* **2000**, *113*, 10486−10504.
(27) Mitani, M.; Mori, H.; Takano, Y.; Yamaki, D.; Yoshioka, Y.; Yamaguchi, K. *J. Chem. Phys.* **2000**, *113*, 4035−4051.
(28) Mitani, M.; Takano, Y.; Yoshioka, Y.; Yamagui, K. *J. Chem. Phys.* **1999**, *111*, 1309−1324.
(29) Ruiz, E.; Alvarez, S.; Cano, J.; Polo, V. *J. Chem. Phys.* **2005**, *123*, 164110/164111−164110/164117.
(30) Albores, P.; Slep, L. D.; Weyhermuller, T.; Rentschler, E.; Baraldo, L. M. *J. Chem. Soc., Dalton Trans.* **2006**, 948−954.
(31) Whangbo, M.-H.; Koo, H.-J.; Dai, D. *J. Solid State Chem.* **2003**, *176*, 417−481.

configuration with the largest coupling predicted by the calculations.

Long-range magnetic ordering, however, is quite unexpected and unusual. Both the cusp in the magnetic susceptibility data and the λ-like anomaly in the heat capacity measurements unambiguously confirm this long-range order and assign $T_c = 18$ K. However, the magnetic structure of $La_3Re_2O_{10}$ remains elusive. Unpolarized powder neutron diffraction data at 4 and 285 K showed no discernible difference, which is attributed to the very dilute and delocalized nature of the spin density in this material. Thus, the nature of the long-range order cannot be determined from the existing neutron data.

It is worth noting that the magnetic properties revealed in this investigation do not agree with the preliminary magnetic susceptibility measurements reported previously,[8] which found an unusually high effective magnetic moment of about 6 μ_B at room temperature. Using the Curie constant from the fit to the high-temperature magnetic susceptibility data collected in this research, an effective moment of 1.25(1) μ_B can be calculated. This value is much closer to the calculated spin-only effective moment for a spin 1/2 system of 1.73 μ_B.

In conclusion, $La_3Re_2O_{10}$ is an interesting magnetic oxide, given that the unpaired electron is extensively delocalized over the $[Re_2O_{10}]^{9-}$ dimeric unit. In spite of long interdimer distances, short-range antiferromagnetic correlations are evident below 200 K and long-range antiferromagnetic order sets in below 18 K.

Acknowledgment. H.L.C. thanks Dr. Paul Dube for his assistance with the heat capacity measurements, Dr. Maggie Austen for useful discussions of the bonding in the Re_2O_{10} dimer, and NSERC for a doctoral Post-Graduate Scholarship. J.E.G. thanks NSERC for financial support. I.V.B. acknowledges NSERC, OIT, and CFI for funding.

IC701011R